Research report

Magnetic resonance spectroscopic analysis of Alzheimer's disease mouse brain that express mutant human APP shows altered neurochemical profile

Alpaslan Dedeoglu[a,b,*], Ji-Kyung Choi[c], Kerry Cormier[a,b],
Neil W. Kowall[a,b], Bruce G. Jenkins[c]

[a] Geriatric Research Education and Clinical Center, Bedford Veterans Administration Medical Center, Bedford, MA 01730, USA
[b] Department of Neurology, Boston University School of Medicine, Boston, MA 02118, USA
[c] Department of Radiology, Massachusetts General Hospital and Harvard Medical School, Boston, MA 02114, USA

Abstract

Transgenic mice that express mutant human amyloid precursor protein (APP_{Tg2576}) develop β-amyloid (Aβ) plaques throughout the cortex starting at 10–12 months of age. We examined the neurochemical profile of APP_{Tg2576} mice using in vitro and in vivo magnetic resonance spectroscopy (MRS); gross abnormalities using magnetic resonance imaging (MRI) and plaque distribution; size and number using immunohistochemistry. Transgenic mice were anesthetized with halothane and scanned at 4.7 T using T2-weighted imaging and in vivo MRS of frontal cortex. In vitro MRS was run from brain extracts of frontal cortex in both APP and wild-type mice. Mice were also perfused and brains were collected and cut for immunohistochemistry. We found that N-acetylaspartate (NAA), glutamate and glutathione were decreased by 17%, 22% and 36%, respectively, in the cerebral cortex of APP transgenic mice at 19 months of age when Aβ deposits are widespread. Taurine was increased 21% compared to wild-type. Decreased levels of NAA and increased levels of taurine are consistent with decreased neuronal viability and increased glial volume, and are similar to findings of decreased NAA and increased myo-inositol in human Alzheimer's disease (AD) brains. Correlation between the severity of Aβ deposition and altered neurochemical profile remains to be studied. Nevertheless, the altered neurochemical profile may be a valuable marker to test therapeutics in this mouse model.
© 2004 Elsevier B.V. All rights reserved.

Keywords: Alzheimer's disease; β-Amyloid; Magnetic resonance imaging; Magnetic resonance spectroscopy; Immunohistochemistry

1. Introduction

Alzheimer's disease (AD) is an age-dependent neurodegenerative disorder that causes a progressive decline in cognitive function. The neuropathological hallmarks of AD are senile plaques, that contain β-amyloid (Aβ) peptide and neurofibrillary tangles, composed of filamentous aggregates of hyperphosphorylated tau protein [30]. AD is a complex, multifactorial disease in which several genes act independently or in concert with each other and/or with environmental agents resulting in amyloid deposition in the brain, neurofibrillary tangle formation and cell death. The deposition of amyloid follows a specific spatial and temporal pattern. Whether amyloid plaques represent a primary or secondary event in AD has been an area of contention.

Development of mouse models has been a critical milestone in AD research making it possible to study the mechanisms of the disease as well as testing therapeutics. Mutations in the APP and PS-1 (presenilin-1) genes are linked to familial AD [14,25,28]. The "Swedish" APP mutation affects the β-secretase cleavage site of the Aβ domain, leading to increased brain production of both $Aβ_{1-40}$ and $Aβ_{1-42}$ from APP [8,11]. Transgenic mice carrying the human Swedish mutant APP_{Tg2576} have been shown to have elevated brain levels of soluble $Aβ_{1-40}$ and $Aβ_{1-42}$ by 6–8 months of age and to develop Aβ-

* Corresponding author. Geriatric Research Education and Clinical Center, Unit 182B, Bedford Veterans, Affairs Medical Center, 200 Springs Road, Bedford, MA 01730, USA. Tel.: +1-617-687-2943; fax: +1-617-687-3515.

E-mail address: dedeoglu@bu.edu (A. Dedeoglu).

containing neuritic plaques in the neocortex and hippo-campus by 10–16 months of age [13,15,16].

Magnetic resonance spectroscopy (MRS) is a noninvasive technique that permits the quantification of metabolic biomarkers in vivo and in vitro, and has been used to characterize Alzheimer's disease [4,31]. Studies in humans show decreases in *N*-acetylaspartate (NAA, a marker for neuronal number and health) and myo-inositol which may either be a marker for osmotic stress or astrogliosis. Myo-inositol may be an earlier marker of pathological change than NAA in AD because of this. Taurine may serve a role similar to myo-inositol in the rodent brain. This study is designed to examine whether the metabolic profile of APP_{Tg2576} transgenic mouse brain is altered at an age when the Aβ deposits are widespread.

2. Materials and methods

2.1. Mice

Transgenic mice overexpressing the human Aβ with the Swedish mutation [15], APP_{Tg2576}, and wild-type littermate controls were used in the study. Separate sets of age-matched mice (19 ± 2 months of age) were used for NMR and immunohistochemistry experiments.

2.2. Histology/immunohistochemistry

Brains were serially cut at 50 μm on a freezing microtome and stained with cresyl violet to identify histopathological abnormalities. Sections were immunostained for $A\beta_{1-40}$, $A\beta_{1-42}$ to define Aβ deposits and GFAP to define astrocytes. Immuno-cytochemical procedures were performed as previously described [21]. In brief, free-floating sections were incubated overnight in primary antibody followed by PBS washes and incubation in peroxidase-conjugated secondary antibody followed by development using DAB as a chromagen.

2.3. Quantitative analysis of Aβ deposits

Three serial sections per mouse brain were analyzed using Image-Pro Plus version 4.5 (Silver Spring, MD). The most rostral, reference section was at the anterior commisure level (∼ 0.1 mm anterior to bregma) and other two sections were 0.3 mm increments caudal to the first one. The plaque number, mean diameter of the plaques and plaque area were determined in the cerebral cortex of one hemisphere of these three sections. All computer identified plaque profiles were manually verified as plaques and were exported to Microsoft Excel. In addition, the cortex area was measured and plaque size and volume were divided by the cortex area to calculate the plaque density.

2.4. MR spectroscopy and imaging

MR imaging of the mice was performed in conjunction with the spectroscopy at 4.7 T (GE Omega, Freemont, CA) using a 20-mm sinusoidal birdcage coil. Animals were kept warm with a 38 °C circulating water blanket. Animals were anesthetized using 1.5% halothane in an NO_2/O_2 mixture. The dose was monitored from outside the magnet and gas was delivered through an extension line. T2-weighted spin echo MR images (TR/TE 3000/60 ms) were collected with spatial resolution of 0.1×0.2 mm in plane and consecutive 1-mm slices. MR spectroscopy was performed as previously reported [17]. Briefly, voxels were placed centered over the cingulate cortex extending to include sensorimotor cortex (see below). The centering over the cingulate was chosen since this area shows a high plaque density in these mice. We analyzed the partial volume averaging of the voxels by superimposing the voxel we collected over a brain image and then aligned that with a standard mouse brain atlas available on the web (http://www.nervenet.org/mbl/atlas170). Thus, the average voxel from frontal cortex had approximately the following volume components: 3.7% non-brain, 5% corpus callosum, 15.1% cingulate, 15.3% sensory, 21.1% parietal and 39.9% motor cortex. The MRS voxel was a subset of the cortical area sampled for the histopathology, however, since the plaque density is reasonably constant in the sampled cortical sections (with the exception of slightly higher density in the cingulate region), the MRS voxel adequately represents the histopathology data. Voxel sizes were tailored to the size of the brain. Typical voxel sizes were approximately $6 \times 2 \times 3$ mm (ca. 36 μl). Spectra were recorded using a PRESS technique with a TR of 2.2 s and TE values of 144 and 272 ms. Data were
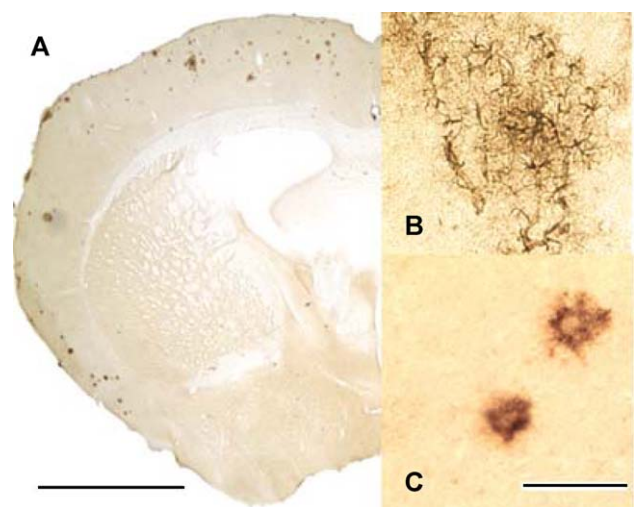

Fig. 1. Representative examples of immunostaining of coronal sections at the level of bregma from APP_{Tg2576} mice at 19 months of age. A (lower magnitude) and C (higher magnitude) show plaques stained by specific antibody $A\beta_{1-40}$ and B (same magnitude as C) is stained by GFAP (a marker for astrocytes). Scale bars: (in A) A, 2 mm; (in C) B,C 10 μm.

Table 1
Size, area and density of plaques that are immunostained by specific antibodies that recognize $A\beta_{1-40}$, $A\beta_{1-42}$ species

	$A\beta_{1-40}$	$A\beta_{1-42}$
Plaque number	197.2 ± 80.5	186.6 ± 54.7
Plaque mean diameter (μm)	2.75 ± 0.3	3.30 ± 0.2
Total plaque area (μm^2)	1524.9 ± 627.2	2263.3 ± 977.5
Plaque number/ctx area ($\times 10^{-6}$)	7.8 ± 3.1	7.4 ± 2.3
Plaque area/ctx area ($\times 10^{-6}$)	60.6 ± 25.9	90.1 ± 39.4

The data is collected from five 19-month-old APP_{Tg2576} transgenic mice hemicortex as explained in detail in Materials and methods. Values are expressed mean ± S.D.

processed using curve fitting of the spectra and intensities were integrated. Resonance integrals were normalized to the creatine peak. Collection of the two TE values allowed for corrections in the T2s of the metabolites that might occur due to differences between the transgenic and wild-type animals. In vitro MRS measurements were made from PCA brain extracts of brain tissue and were run at 11.75 T Bruker spectrometer. Samples were prepared in 99.9% D_2O (pH 7.2) and run at 26 °C. Spectra were analyzed as above for the in vivo spectra.

3. Results and discussion

Coronal sections were immunostained for $A\beta_{1-40}$, $A\beta_{1-42}$ to define $A\beta$ deposits and for GFAP to define astrocytes. GFAP is a marker for astrocytosis that is elevated with age in mammals [22] and is increased in amyloid forming APP transgenic mice [16,24]. A representative picture of the distribution of plaques in the cerebral cortex of one hemisphere (Fig. 1A) and a high magnification picture of plaques stained by specific $A\beta_{1-40}$ antibody (Fig. 1C) together with a picture of plaques stained by GFAP antibody (Fig. 1B) is shown in Fig. 1. The number of plaques, mean diameter and area is calculated in the cerebral cortex of one hemisphere and shown in Table 1.

In vivo MRS of five APP_{Tg2576} and three wild-type mice was performed as described in Materials and methods. The most remarkable differences were increased taurine and decreased NAA in the cortex in the APP mice (Fig. 2B). In the in vivo spectra we found, for APP and WT mice, respectively, that NAA/Cr was 1.30 ± 0.13 vs. 1.47 ± 0.12 ($p = 0.12$); taurine/Cr was 0.31 ± 0.12 vs. 0.21 ± 0.04 ($p = 0.12$); glx (glutamate plus glutamine) was 0.26 ± 0.16
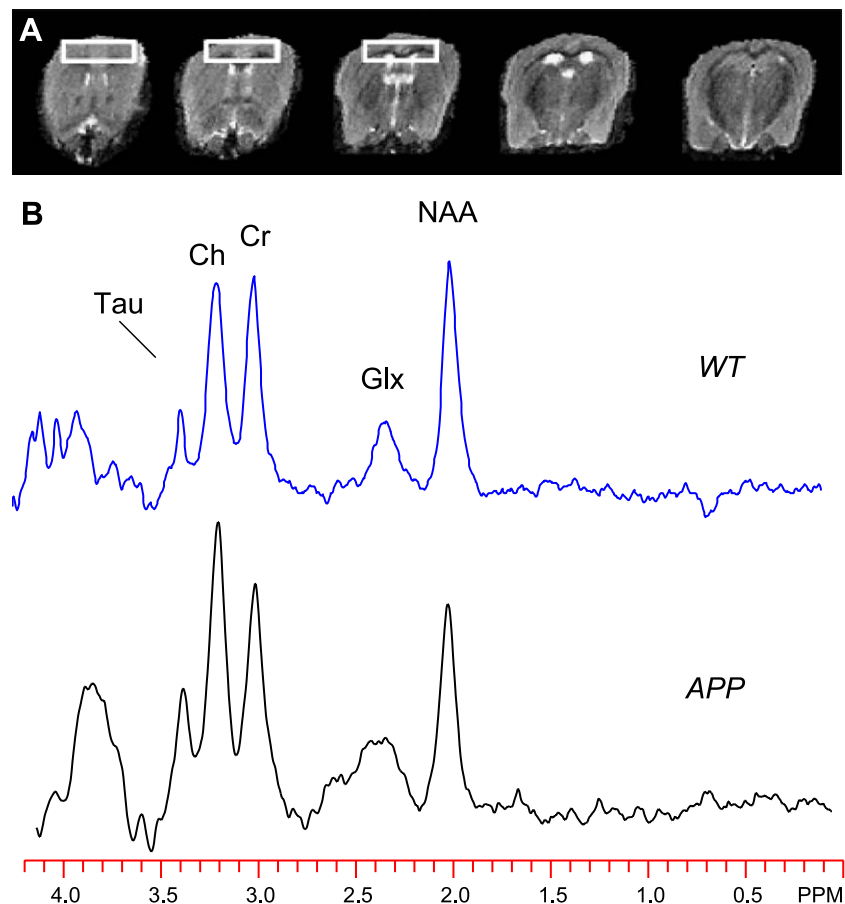

Fig. 2. (A) Representative T2-weighted image showing an APP_{Tg2576} mouse brain. Voxels were placed centered over the cingulate cortex extending to include sensorimotor cortex to perform spectroscopy in the defined area. Voxel sizes were tailored to the size of the brain. Typical voxel sizes were approximately $6 \times 2 \times 3$ mm (ca. 36 μl). (B) Spectra from frontal cortex in wild-type (top) and in an APP_{Tg2576} mouse showing frontal cortex (bottom). There is a decrease in NAA, and an increase in taurine in the APP mice. TR/TE (2200/144 ms).

vs. 0.30 ± 0.10 and Cho/Cr was 1.06 ± 0.22 vs. 0.75 ± 0.24 ($p = 0.07$).

Mice that were studied with in vivo MRS, as well as additional mice, were sacrificed and samples of cortex that corresponded (as closely as possible) to the in vivo voxels were analyzed with in vitro MRS. Representative proton spectra from an APP and wild-type mouse are shown in Fig. 3. A wider range of neurochemicals can be measured by in vitro MRS compared to in vivo MRS as shown in Table 2. Similar to what we observed in the in vivo MRS, NAA is decreased by 17% and taurine levels are increased by 21%. In addition, glutamate, and glutathione levels were decreased by 22% and 37%, respectively. No significant changes were noted in any other chemicals including myo-inositol, a chemical often elevated in studies of human AD cortex [4,31]. Taurine is much more highly concentrated in rodent brain compared to human brain, and the previous data support the role of taurine as an osmoregulator [7], similar to the role that myo-inositol has been conjectured to play in human brain [5,23]. Thus, the increased taurine levels noted in these mice may reflect a similar process to that which occurs with increased myo-inositol in human AD.

A number of studies have shown depleted glutathione levels in AD tissue [1,2,10] and that glutathione cycle impairment is a key event in Aβ-induced cell toxicity [9]. In addition, reduced levels of glutathione are correlated with cognitive impairment [26]. The reductions of glutathione that we observe in the APP mice compared to the age-matched controls thus fit into this idea and suggest that oxidative stress may play a role in the development of the altered metabolic profile we observe. Since normal aging is associated with decreased levels of many anti-oxidants and

increased oxidative damage [3], the interaction between aging and plaque burden may lead to the changes we found.

Numerous studies have shown a decreased NAA in AD cortex [4,20,29,31]. NAA is predominantly an intraneuronal chemical and can be used as marker for neuronal density and/or health [17,27,32,33,34]. Decreased NAA in transgenic APP mice may either suggest neuronal loss or an altered volume ratio of neuron to other cells such as microglia and/or astrocytes which are known to be increased in the presence of Aβ plaques and related neuroinflammation.

Our immunohistochemical analysis of brains of APP mice using GFAP antibody to identify astrocytes is consistent with

Table 2
In vitro MRS results showing the metabolite changes in APP$_{Tg2576}$ and wild-type control mice

Chemical	WT ($n = 10$)	APP$_{Tg2576}$ ($n = 9$)	% Change	
Myo-inositol	0.52 ± 0.08	0.58 ± 0.12		
Taurine	0.67 ± 0.14	0.81 ± 0.17	20.80	$p < 0.05$
Scyllo-inositol	0.10 ± 0.08	0.05 ± 0.04		
Choline	0.83 ± 0.22	0.77 ± 0.19		
Cr–CH3	1	1		
GSH	0.19 ± 0.06	0.12 ± 0.06	−36.80	$p < 0.05$
Aspartate	0.14 ± 0.09	0.12 ± 0.13		
Glutamine	0.40 ± 0.09	0.40 ± 0.10		
Succinate	0.07 ± 0.02	0.07 ± 0.02		
Glutamate	0.99 ± 0.11	0.77 ± 0.16	−22.20	$p < 0.01$
NAA	0.86 ± 0.10	0.71 ± 0.12	−17.40	$p < 0.05$
GABA	0.23 ± 0.08	0.20 ± 0.05		
Alanine	0.15 ± 0.07	0.11 ± 0.06		
Lactate	0.65 ± 0.05	0.59 ± 0.15		

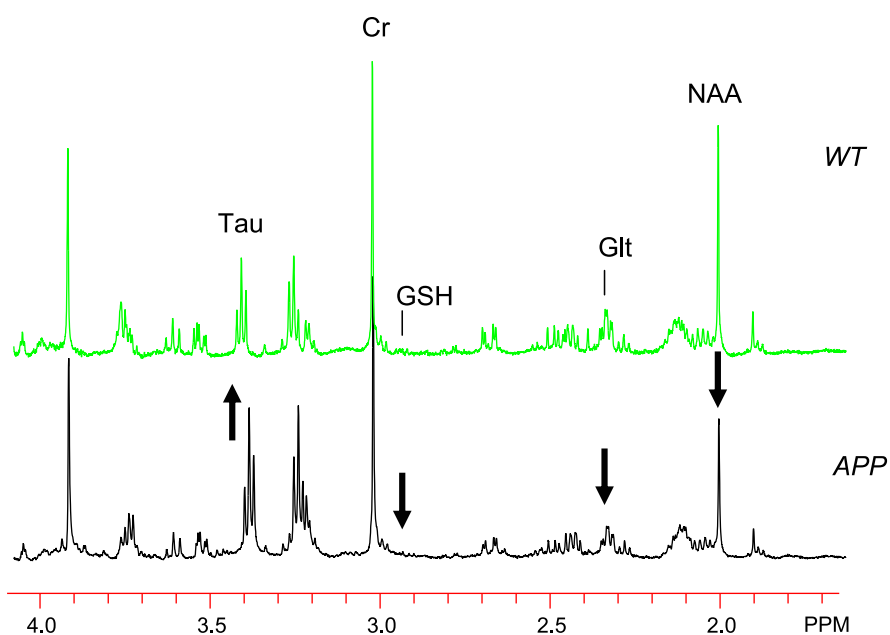Values are expressed mean $\pm$ S.D. p-value compared to wild-type vs. APP mice.

Fig. 3. Representative high resolution in vitro MR spectroscopy taken at 500 MHz from extracts of cortex from an APP transgenic mouse and a littermate wild-type. A large number of neurochemicals can be measured using this method. Significant changes are shown with arrows going up or down. NAA, *N*-acetylaspartate; glt, glutamate; gsh, glutathione; tau, taurine.

the presence of activated astrocytes. Likewise, taurine, which is predominantly present in the glia, was higher in APP transgenic mice compared to the same age wild-type mice in both in vivo and in vitro MRS studies. Histological analysis and MR analysis were performed in two separate sets of mice since tissue collection was completely different in two procedures. Therefore, there was no way to correlate the findings in the same mice. It is not possible to draw conclusions since no correlation analysis is provided in this study. However, our preliminary observations in another mouse model (APPxPS-1) that express comparable amounts of plaque pathology at a younger age suggest that similar amounts of plaques are not accompanied with similar changes in younger and older mice [12]. Conclusive results require further studies at multiple ages. It is known that astrogliosis is related to aging and that GFAP is increased by aging [22]. Astrogliosis is also related to plaque formation [16,24]. Our studies on 19-month-old single transgenic APP$_{Tg2576}$ mice and 6-month-old double transgenic APPxPS-1 mice suggest that plaques themselves are not enough to cause similar neurochemical changes since both of these models develop plaques in similar quantities at different ages. It is possible that in addition to plaque formation, age is a very important factor in causing an altered neurochemical profile in the brains of mice. Numerous studies have suggested changes in chemicals measurable by MRS such as cholines and NAA which occur as a result of normal aging in both humans and rodents [6,18,19]. Thus, the interaction between normal aging and expression of plaques may accelerate the changes that occur as a consequence of normal aging.

Acknowledgements

References

[1] A.Y. Abramov, L. Canevari, M.R. Duchen, Changes in intracellular calcium and glutathione in astrocytes as the primary mechanism of amyloid neurotoxicity, J. Neurosci. 23 (2003) 5088–5095.

[2] J.S. Bains, C.A. Shaw, Neurodegenerative disorders in humans: the role of glutathione in oxidative stress-mediated neuronal death, Brain Res. Brain Res. Rev. 25 (1997) 335–358.

[3] M.F. Beal, Oxidatively modified proteins in aging and disease, Free Radic. Biol. Med. 32 (2002) 797–803.

[4] W. Block, F. Traber, S. Flacke, F. Jessen, C. Pohl, H. Schild, In-vivo proton MR-spectroscopy of the human brain: assessment of *N*-acetylaspartate (NAA) reduction as a marker for neurodegeneration, Amino Acids 23 (2002) 317–323.

[5] A. Brand, C. Richter-Landsberg, D. Leibfritz, Multinuclear NMR studies on the energy metabolism of glial and neuronal cells, Dev. Neurosci. 15 (1993) 289–298.

[6] J.C. Brooks, N. Roberts, G.J. Kemp, M.A. Gosney, M. Lye, G.H. Whitehouse, A proton magnetic resonance spectroscopy study of age-related changes in frontal lobe metabolite concentrations, Cereb. Cortex 11 (2001) 598–605.

[7] M.B. Burg, E.D. Kwon, D. Kultz, Regulation of gene expression by hypertonicity, Annu. Rev. Physiol. 59 (1997) 437–455.

[8] X.D. Cai, T.E. Golde, S.G. Younkin, Release of excess amyloid beta protein from a mutant amyloid beta protein precursor, Science 259 (1993) 514–516.

[9] S.M. Cardoso, C.R. Oliveira, Glutathione cycle impairment mediates A beta-induced cell toxicity, Free Radic. Res. 37 (2003) 241–250.

[10] C. Cecchi, S. Latorraca, S. Sorbi, T. Iantomasi, F. Favilli, M.T. Vincenzini, G. Liguri, Gluthatione level is altered in lymphoblasts from patients with familial Alzheimer's disease, Neurosci. Lett. 275 (1999) 152–154.

[11] M. Citron, T. Oltersdorf, C. Haass, L. McConlogue, A.Y. Hung, P. Seubert, C. Vigo-Pelfrey, I. Lieberburg, D.J. Selkoe, Mutation of the beta-amyloid precursor protein in familial Alzheimer's disease increases beta-protein production, Nature 360 (1992) 672–674.

[12] A. Dedeoglu, J. Choi, K. Cormier, S.A. Matson, B.G. Jenkins, N.W. Kowall, Ibuprofen reduces Aβ(1−42)/Aβ(1−40) ratio in Alzheimer mice cortex at ages where no metabolic changes are noted by magnetic resonance spectroscopy, Society for Neuroscience, 2003, Online Program No. 203.9, 2003 Abstract Viewer/Itinerary Planner, Washington, DC, 2003.

[13] S.A. Frautschy, F. Yang, M. Irrizarry, B. Hyman, T.C. Saido, K. Hsiao, G.M. Cole, Microglial response to amyloid plaques in APPsw transgenic mice, Am. J. Pathol. 152 (1998) 307–317.

[14] J. Hardy, Amyloid, the presenilins and Alzheimer's disease, Trends Neurosci. 20 (1997) 154–159.

[15] K. Hsiao, P. Chapman, S. Nilsen, C. Eckman, Y. Harigaya, S. Younkin, F. Yang, G. Cole, Correlative memory deficits, Abeta elevation, and amyloid plaques in transgenic mice, Science 274 (1996) 99–102.

[16] M.C. Irizarry, M. McNamara, K. Fedorchak, K. Hsiao, B.T. Hyman, APPSw transgenic mice develop age-related A beta deposits and neuropil abnormalities, but no neuronal loss in CA1, J. Neuropathol. Exp. Neurol. 56 (1997) 965–973.

[17] B.G. Jenkins, P. Klivenyi, E. Kustermann, O.A. Andreassen, R.J. Ferrante, B.R. Rosen, M.F. Beal, Nonlinear decrease over time in *N*-acetyl aspartate levels in the absence of neuronal loss and increases in glutamine and glucose in transgenic Huntington's disease mice, J. Neurochem. 74 (2000) 2108–2119.

[18] K. Kantarci, G.E. Smith, R.J. Ivnik, R.C. Petersen, B.F. Boeve, D.S. Knopman, E.G. Tangalos, C.R. Jack Jr., 1H magnetic resonance spectroscopy, cognitive function, and apolipoprotein E genotype in normal aging, mild cognitive impairment and Alzheimer's disease, J. Int. Neuropsychol. Soc. 8 (2002) 934–942.

[19] R. Katz-Brull, A.R. Koudinov, H. Degani, Choline in the aging brain, Brain Res. 951 (2002) 158–165.

[20] W.E. Klunk, K. Panchalingam, J. Moossy, R.J. McClure, J.W. Pettegrew, *N*-acetyl-L-aspartate and other amino acid metabolites in Alzheimer's disease brain: a preliminary proton nuclear magnetic resonance study, Neurology 42 (1992) 1578–1585.

[21] N.W. Kowall, P. Hantraye, E. Brouillet, M.F. Beal, A.C. McKee, R.J. Ferrante, MPTP induces alpha-synuclein aggregation in the substantia nigra of baboons, NeuroReport 11 (2000) 211–213.

[22] N.J. Laping, B. Teter, N.R. Nichols, I. Rozovsky, C.E. Finch, Glial fibrillary acidic protein: regulation by hormones, cytokines, and growth factors, Brain Pathol. 4 (1994) 259–275.

[23] R.O. Law, Regulation of mammalian brain cell volume, J. Exp. Zool. 268 (1994) 90–96.

[24] G.P. Lim, F. Yang, T. Chu, P. Chen, W. Beech, B. Teter, T. Tran, O. Ubeda, K.H. Ashe, S.A. Frautschy, G.M. Cole, Ibuprofen suppresses plaque pathology and inflammation in a mouse model for Alzheimer's disease, J. Neurosci. 20 (2000) 5709–5714.

[25] P. Malherbe, J.G. Richards, J.R. Martin, H. Bluethmann, J. Maggio, G. Huber, Lack of beta-amyloidosis in transgenic mice expressing low levels of familial Alzheimer's disease missense mutations, Neurobiol. Aging 17 (1996) 205–214.

[26] A. McCaddon, P. Hudson, D. Hill, J. Barber, A. Lloyd, G. Davies, B. Regland, Alzheimer's disease and total plasma aminothiols, Biol. Psychiatry 53 (2003) 254–260.

[27] B.L. Miller, A review of chemical issues in 1H NMR spectroscopy: N-acetyl-L-aspartate, creatine and choline, NMR Biomed. 4 (1991) 47–52.

[28] D.L. Price, S.S. Sisodia, Mutant genes in familial Alzheimer's disease and transgenic models, Annu. Rev. Neurosci. 21 (1998) 479–505.

[29] N. Schuff, D.L. Amend, D.J. Meyerhoff, J.L. Tanabe, D. Norman, G. Fein, M.W. Weiner, Alzheimer disease: quantitative H-1 MR spectroscopic imaging of frontoparietal brain, Radiology 207 (1998) 91–102.

[30] D.J. Selkoe, Alzheimer's disease: genes, proteins, and therapy, Physiol. Rev. 81 (2001) 741–766.

[31] T.K. Shonk, R.A. Moats, P. Gifford, T. Michaelis, J.C. Mandigo, J. Izumi, B.D. Ross, Probable Alzheimer disease: diagnosis with proton MR spectroscopy, Radiology 195 (1995) 65–72.

[32] M.L. Simmons, C.G. Frondoza, J.T. Coyle, Immunocytochemical localization of N-acetyl-aspartate with monoclonal antibodies, Neuroscience 45 (1991) 37–45.

[33] G. Tsai, J.T. Coyle, N-acetylaspartate in neuropsychiatric disorders, Prog. Neurobiol. 46 (1995) 531–540.

[34] J. Urenjak, S.R. Williams, D.G. Gadian, M. Noble, Specific expression of N-acetylaspartate in neurons, oligodendrocyte-type-2 astrocyte progenitors, and immature oligodendrocytes in vitro, J. Neurochem. 59 (1992) 55–61.